THE JOURNAL OF PHYSICAL CHEMISTRY B

Article

pubs.acs.org/JPCB

Mechanistic Investigation of Interactions between Steroidal Saponin Digitonin and Cell Membrane Models

Nataliya Frenkel,[†,‡,#] Ali Makky,[†,#,⊥] Ikhwan Resmala Sudji,[§] Michael Wink,*[,§] and Motomu Tanaka*[,†,‡,∥]

[†]Physical Chemistry of Biosystems, Institute of Physical Chemistry and [§]Institute of Pharmacy and Molecular Biotechnology, Heidelberg University, D69120 Heidelberg, Germany

[‡]Institute for Toxicology and Genetics, Karlsruhe Institute for Technology, D76021, Karlsruhe, Germany

[∥]Institute for Integrated Cell-Material Sciences (WPI iCeMS), Kyoto University, 606-8501 Kyoto, Japan

ABSTRACT: Digitonin is an amphiphilic steroidal saponin, a class of natural products that can bind to cholesterol and lyse cells. Despite the known cell membrane lysis activity, it remains unclear how it interacts with cell membranes. In the present work, the interaction mechanism between digitonin and cell membrane models has quantitatively been investigated using a combination of physical techniques. It has been demonstrated that digitonin molecules bind specifically to cholesterol in the membrane, resulting in the formation of cholesterol−digitonin complexes on the membrane surface by removing cholesterol from the membrane core. Changes in the mass density and the film mechanics caused by the digitonin were determined by using quartz crystal microbalance with dissipation (QCM-D), and the combination of X-ray reflectivity (XRR) and dual polarization interferometry (DPI) yielded the hydration level of the cholesterol−digitonin complexes. From differential scanning calorimetry (DSC) analysis, supporting evidence was obtained that cholesterol was removed from the membrane core.

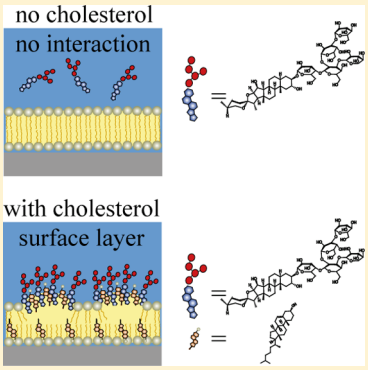

INTRODUCTION

Saponins represent an important class of bioactive secondary metabolites produced mainly by plants that serve as natural defense compounds against herbivores and microbial infections.[1] Saponins are present in many medicinal plants that have been used as anti-inflammatory, secretolytic, antifungal, antibacterial, cholesterol-lowering, anticancer drugs, and an adjuvant for vaccinations.[2] Chemically, saponins are either triterpenes or steroids,[3,4] which can carry one or several hydrophilic oligosaccharide chains connected to the aglycone via glycosidic or ester bonds.[4] In plants, saponins are stored in the vacuole as inactive bidesmosides that carry at least two sugar chains. When a plant is wounded or infected, a glucosidase or esterase is released, which cleaves one of the sugar chains producing the bioactive amphiphilic monodesmosides.[5] Such an amphiphilic nature of many saponin derivatives results in a strong surface activity, which can be used to make cell membranes permeable to allow for the access of various small molecules to nuclei and intracellular organelles.[6] Higher concentrations of monodesmosidic saponins completely lyse cells, which can easily be demonstrated using red blood cells. Digitonin, one of the steroidal saponins found in *Digitalis* species, has been widely used for the cell membrane permeabilization. Although other commonly used agents, such as Triton, glycerol, and toluene, interact nonspecifically with cell membranes,[7] accumulating evidence suggests that digitonin specifically interacts with membrane sterols.[8,9] The increase in the permeability of ions,[10] metabolites,[10,11] and enzymes[11] across cell membranes can be attributed to the decrease in the packing of hydrocarbon chains caused by the removal of sterols, which fill defects and free voids in the hydrophobic membrane core. The higher selectivity of digitonin activity toward cell membranes than organelles[1,12] actually seems plausible if one considers the fact that cholesterol and other 3-hydroxysterols are present at high molar ratios in cell membranes.[7]

In previous studies,[12−14] it has been suggested that digitonin at low concentration (0.001 wt %) leads to the vesiculation and pore formation in cell membranes, resulting in the leakage of ions, small molecules, and proteins. For example, ESR[14] and electrophysiology measurements[15] suggested the incorporation of digitonin into cholesterol-free lipid membranes. A recent study[16] reported that all steroid saponins form films with negligibly a small viscoelastic modulus. However, the mechanistic understanding of the mode of interactions between digitonin and cell membranes is still missing.

The primary aim of this study is to quantitatively determine how digitonin interacts with cell membrane models in the presence and absence of cholesterol. To achieve this goal, we deposited planar phospholipid membranes on solid substrates (called supported membranes)[17,18] with and without cholesterol. The amount (mass density) of digitonin and the change in film mechanics caused by digitonin were determined by using quartz crystal microbalance with dissipation (QCM-D). The combination with dual polarization interferometry (DPI) enabled us to monitor the change in chain packing (refractive

Received: July 25, 2014
Revised: October 21, 2014
Published: November 20, 2014

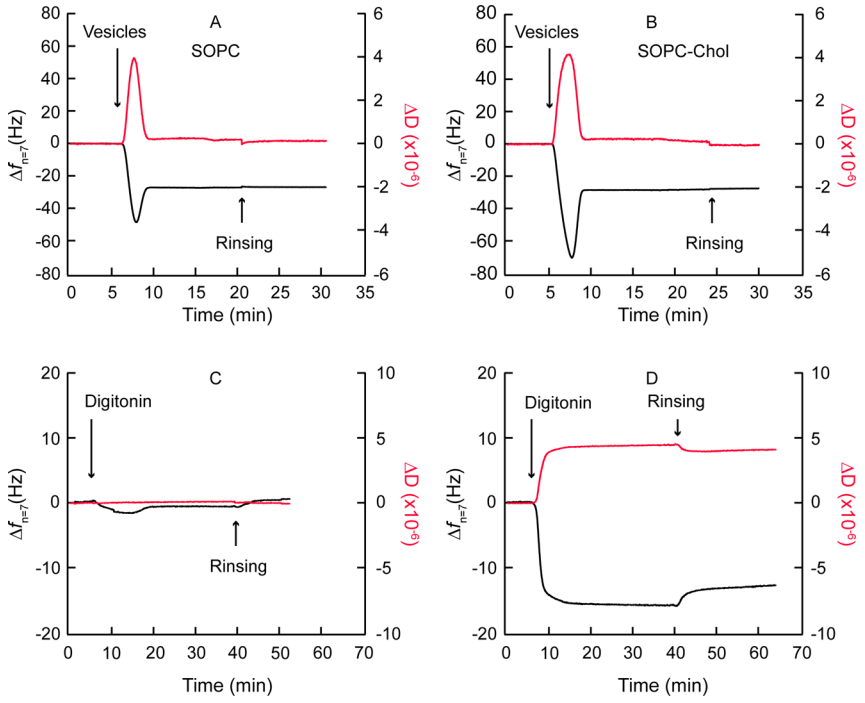

Figure 1. Δf and ΔD of (A) a pure SOPC membrane and (B) a SOPC membrane incorporating 20 mol % cholesterol at 35 MHz in the absence of digitonin. Although the injection of 50 μM digitonin did not lead to any remarkable change in the SOPC membrane (C), the membrane with cholesterol (D) exhibited abrupt changes in both Δf and ΔD upon the injection of 50 μM digitonin.

index and birefringence) and the degree of hydration. Moreover, X-ray reflectivity (XRR) and differential scanning calorimetry (DSC) in the presence and absence of cholesterol unraveled the impact of digitonin on the membrane fine structures and membrane thermodynamics, respectively. Details of the obtained results are discussed in the following sections.

EXPERIMENTAL METHODS

Synthetic Reagents. 1-Stearoyl-2-oleoyl-*sn*-glycero-3-phosphocholine (SOPC, 99% pure, MW = 788.14 g/mol) and cholesterol (99% pure, MW = 386.66 g/mol) were purchased from Avanti Polar Lipids (Alabaster, U.S.A.), while digitonin (MW = 1229.31 g/mol) and phosphate buffered saline (2.7 mM KCl and 137 mM NaCl, pH 7.4) were from Sigma-Aldrich (Munich, Germany). Ultrapure water (Millipore, Molsheim, France) with a resistivity of 18.2 MΩ·cm was used in all experiments.

Sample Preparation. Small unilamellar vesicles (SUVs) of SOPC and SOPC−cholesterol (80/20, mol %) were prepared according to Bangham's method[19] followed by the sonication of vesicle suspensions; phospholipid stock solutions in chloroform/methanol (9:1 v/v) were evaporated for 3 h under reduced pressure with a rotary evaporator, and the resulting dry lipid film was hydrated at 40 °C with PBS buffer (10 mM, pH, 7.4) to obtain a final lipid concentration of 2 mM.[20] Then, the lipid suspension was sonicated for 45 min with a titanium tip sonicator S3000 (Misonix, Farmingdale, NY, U.S.A.). Afterward, the suspension was centrifuged at 10000 rpm at 4 °C for 30 min to remove any residual titanium particles from the tip sonicator.

DSC. DSC measurements were carried out using a VP-DSC calorimeter (MicroCal, Inc., Northampton, MA, U.S.A.). To ensure that thermal equilibrium was reached, three successive heating/cooling scans were recorded between 2 and 15 °C at a scan rate of 5 °C/h. The samples used for the DSC measurements were prepared as 2 mM lipid suspensions of SOPC membranes containing, 0, 5, and 20 mol % of cholesterol, suspended in PBS. To monitor the interaction with digitonin, vesicle suspensions were incubated with 50 μM digitonin for 30 min before starting the measurements.

QCM-D. QCM-D measurements were performed with a QCM-D E4 (Q-Sense, Gothenburg, Sweden). SUV suspensions (0.2 mM in PBS) were deposited on AT-cut SiO_2-coated quartz crystals with a fundamental frequency of 5 MHz for ∼10 min, followed by rinsing with PBS buffer for 15 min. After confirming the membrane formation, digitonin solution (50 μM in PBS) was injected for 10 min and allowed to adsorb for another 20 min. Finally, the crystal was washed with PBS for 15 min. The peristaltic pump for liquid flow was set to 100 μL/min, and the temperature was stabilized at 25 ± 0.1 °C.

If the adsorbed layer is homogeneous and rigid, the shift of resonant frequency (Δf) is proportional to the adsorbed mass per unit surface (Δm) as described by the Sauerbrey[21] equation

$$\Delta m = -\frac{C\Delta f}{n}$$

where C is the mass sensitivity constant of the quartz (C = 17.7 ng/cm^2 Hz at f = 5 MHz) and n is the overtone number. However, if the adsorbed layer is decoupled from the quartz oscillation due to its viscoelasticity, the Sauerbrey equation is invalid due to an increase in energy dissipation. For such a case, the mechanical properties of the layer are represented by a parallel combination of a spring and a dashpot (Voigt−Voinova model[22])

$$G^* = G' + iG'' = \mu_f + 2\pi i f \eta_f = \mu_f(1 + 2\pi i f \tau_f)$$

where G^* is a complex modulus and G' and G'' are storage and loss moduli, respectively. f is the oscillation frequency, μ_f the

dx.doi.org/10.1021/jp5074939 | J. Phys. Chem. B 2014, 118, 14632−14639

elastic shear modulus, η_f the shear viscosity, and τ_f the characteristic relaxation time of the film, $\tau_f = \eta_f/\mu_f$.

In the present work, three overtones (third, fifth, and seventh) were used to model the viscoelastic properties of the adsorbed layer of digitonin using Q-TOOLS software (version 3.0.15, QSense, Gothenburg, Sweden), assuming a fluid viscosity of η = 1 mPa s and fluid density of ρ_{bulk} = 1000 kg/m^3. Throughout the fitting, the range of each parameter was confined as follows: (i) η = 0.5−10 mPa s, (ii) $\mu = 10^4$−10^8 Pa, and (iii) ρ = 1000−1800 kg/m^3. It should be noted that the layer thickness used for the fit was obtained by XRR experiments (see the next section).

High-Energy Specular XRR. XRR measurements were performed at a sealed X-ray tube (D8 Advance, Bruker, Germany), operating with Mo $K\alpha$ radiation (E = 17.48 keV, λ = 0.0709 nm). The incident beam was collimated by various slits, reducing the beam size to 200 μm in the scattering plane. Automatic attenuator settings were used to avoid radiation damage. The scans were completed in approximately 3 h. Prior to the membrane deposition, the cleaned Si wafers were placed into a Teflon chamber with Kapton windows. The momentum transfer perpendicular to the membrane plane is given as a function of the angle of incidence α_i, $q_z = (4\pi/\lambda) \sin \alpha_i$.

For each measurement point, the reflectivity was corrected for the beam footprint and for the beam intensity with the aid of an in-beam monitor. The data were fitted by using the Parratt formalism[23,24] with a genetic minimization algorithm implemented in the Motofit software package.[25]

DPI. DPI measurements were performed at T = 25 ± 0.1 °C with the *Ana*light BIO200 (Farfield Group Ltd., United Kingdom), using a dual slab waveguide chip with four layers of SiO_xN_y (22 mm × 6 mm) illuminated with an alternating polarized laser beam (wavelength = 632.8 nm). The deposition of a film with a distinct refractive index n and thickness d within the evanescent field generated by transverse electric (TE) and transverse magnetic (TM) waveguide modes causes a relative phase shift corresponding to shift of the interference patterns.[26−28]

Prior to each set of measurements, the baseline was defined by calibrating the chip with ethanol (80%) and pure water. Vesicle suspensions (1.4 mM) were infused at a flow rate of 5 μL/min with a syringe pump followed by rinsing with buffer at the same flow rate. Digitonin solutions (50 μM) were infused at a flow rate of 4 μL/min. After the incubation for 1 h, the sample was rinsed at the same flow rate.

RESULTS AND DISCUSSION

QCM-D. Figure 1A and B represents the change in Δf and ΔD during the formation of supported membranes in the absence and presence of 20 mol % cholesterol, respectively. An abrupt decrease in the frequency (Δf_{SOPC} = −50 Hz and $\Delta f_{SOPC\text{-}Chol}$ = −68 Hz) and an increase in the dissipation ($\Delta D_{SOPC} = 3.7 \times 10^{-6}$ and $\Delta D_{SOPC\text{-}Chol} = 4.1 \times 10^{-6}$) suggest the adsorption of lipid vesicles.[29] Once a critical density of adsorbed vesicles was reached, the fusion of vesicles into planar membranes could be monitored by an increase in Δf and a decrease in ΔD due to the release of water from the inner space of vesicles. This resulted in the saturation levels, Δf = −26 Hz and $\Delta D = 0.01 \times 10^{-6}$ for both systems, indicating the formation of a stable supported membrane.[29]

The injection of a 50 μM digitonin solution to the pure SOPC membrane (Figure 1C) did not cause any remarkable change in both Δf ($\Delta f_{n=7} \approx -1$ Hz) or ΔD ($\sim 0.07 \times 10^{-6}$), suggesting that the SOPC membrane remains almost intact in the presence of digitonin. In contrast, the injection of digitonin to the SOPC membrane containing 20 mol % cholesterol (Figure 1D) led to a significant decrease in Δf ($\Delta f_{n=7} \approx -15.5$ Hz) and an increase in ΔD ($\sim 5 \times 10^{-6}$). The abrupt change in Δf can be attributed to the increased effective mass caused by the adsorption of digitonin molecules. In addition, the simultaneous increase in ΔD indicates an increase in the membrane viscosity due to the adsorption or insertion of digitonin molecules. It is notable that both Δf and ΔD did not come back to the initial levels after rinsing with PBS buffer at t = 30 min. Our experimental finding implies that the interaction of digitonin with membranes is irreversible and specifically driven by the presence of cholesterol. This seems consistent with previous accounts,[1,9,14,15] where it was attributed to a hydrophobic interaction between the aglycone part of digitonin and cholesterol molecules.

To further understand the mode of interaction between digitonin and membranes with cholesterol, the normalized changes in frequency (Δf) and dissipation (ΔD) for the three overtones (n = 3, 5, 7) were plotted (Figure 2). The fact that

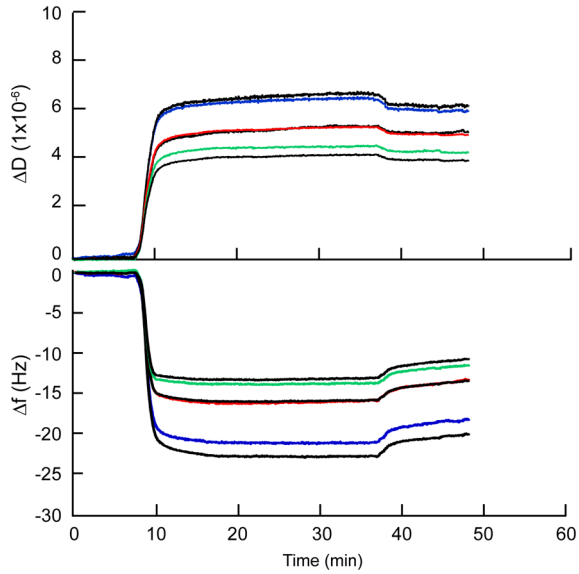

Figure 2. Normalized change in frequency (Δf_n) and dissipation (ΔD) as a function of time, recorded for the three overtones (blue: n = 3; red: n = 5; and green: n = 7; f_0 = 5 MHz). The black lines correspond to the best fits based on the Voigt model for the three overtones. $h_0 = 3.34 \times 10^{-4}$ m; ρ_0 = 2650 kg/m^3; ρ_2 = 1000 kg/m^3; and $\eta_2 = 1 \times 10^{-3}$ kg/m·s. T = 25.0 ± 0.1 °C.

no overlap could be observed indicates that the adsorbed digitonin molecules form a viscous layer on the membranes with cholesterol or significantly alter the mechanical characteristics of membranes. Thus, the calculation of the adsorbed mass of digitonin within the framework of the Sauerbrey equation is obviously invalid as this assumes that the normalized changes in frequency (Δf) should be independent of overtones.

As a more realistic model to describe the membrane mechanics, we fitted the experimental results in Figure 2 using the Voigt−Voinova model. The best-fit results (black broken lines) yield the change in adsorbed mass, the shear modulus (μ_1), and shear viscosity (η_1). Excellent agreement between the fitting results and the measured data for all three overtones gives supporting evidence about the validity of the

dx.doi.org/10.1021/jp5074939 | J. Phys. Chem. B 2014, 118, 14632−14639

model, yielding $\Delta m_{QCM\text{-}D} \approx 735$ ng/cm^2 and a density of ~1638 kg/m^3 for the digitonin layer. It should be noted that the layer thickness used for the fit was obtained by XRR experiments and set to be 45 Å. The obtained parameters from the best-fit models are summarized in Table 1.

Table 1. Modeled Parameters from QCM-D for the Supported Planar Bilayer and for Digitonin Layer

layer	Δm [ng/cm^2]	d [Å]	ρ [g/cm^3]	η [mPa·s]	μ [kPa]
digitonin	735 ± 45	45[a]	1.64 ± 0.10	1.1 ± 0.1	70 ± 6
SOPC–chol	490 (465 ± 20)[b]	47[a]	1.05	>10	>1000

[a]A constant thickness obtained from XRR was taken for the calculation. [b]The mass value within parentheses refers to the Sauerbrey equation using n = 7, that is, 35 MHz.

It should be noted that the shear viscosity of the digitonin layer, ~1 mPa·s, is comparable to that of water (1 mPa·s) and 10 times lower than that of the supported membranes (>20 mPa·s).[30] This might be correlated to the hydrating water coupled to five sugar moieties of digitonin, which was also reported for highly hydrated proteins[31] and DNA.[30] However, despite good agreement between the simple mechanical model and the experimental data, the validation of the model requires supporting evidence from structural characterizations.

High-Energy Specular XRR. To resolve the fine structures of supported membranes interacting with digitonin, we measured specular XRR at a high energy (17.48 keV) at the solid/liquid interface. Figure 3a shows the XRR curves of a SOPC membrane before (black) and after (red) incubation with 50 μM digitonin for 1 h, together with the best-fit results to the experimental results (solid lines). The curves were fitted with five-slab model, including outer head groups, alkyl chains, inner head groups, water reservoir, and SiO_2. The global shapes of curves as well as the fitting results are almost identical, indicating that digitonin causes no remarkable change in the structural integrity of the SOPC membrane, such as thickness d, SLD, and root-mean-square (rms) roughness σ of each region (Table 2).

In contrast, XRR of a SOPC membrane incorporating 20 mol % cholesterol (black) exhibited a clear change in the global shape after the incubation with 50 μM digitonin for 1 h (red).

Table 2. Best-Fit Parameters ($X^2 \leq 0.05$) for the XRR Results for a Pure SOPC Membrane as Presented in Figure 3B in the Absence and Presence of 50 μm Digitonin

	no digitonin			with digitonin		
SOPC	d [Å]	SLD [10^{-6} Å^{-2}]	σ [Å]	d [Å]	SLD [10^{-6} Å^{-2}]	σ [Å]
outer head group	10.6	11.8	4.5	10.9	11.9	4.9
alkyl chain	24.6	7.4	3.8	23.8	7.3	3.9
inner head group	9.1	11.6	3.3	9.3	11.9	3.9
water	3.1	9.4	3.5	3.3	9.4	3.4
SiO_2	10.1	18.6	3.1	10.1	18.6	3.4

First of all, it should be noted that XRR of the membrane with 20 mol % cholesterol shows a distinct difference from that of a pure SOPC membrane as alkyl chains are in a liquid-ordered phase in the presence of cholesterol.[32,33] New features observed at $q_z < 0.1$ Å^{-1} can better be interpreted as the formation of an "additional layer (slab)", rather than assuming the structural change of the existing membrane (Table 3).

Table 3. Best-Fit Parameters ($X^2 \leq 0.02$) for the XRR Results for a SOPC Membrane Incorporating 20 mol % Cholesterol as Presented in Figure 3B in the Absence and Presence of 50 μm Digitonin

	no digitonin			with digitonin		
SOPC–chol	d [Å]	SLD [10^{-6} Å^{-2}]	σ [Å]	d [Å]	SLD [10^{-6} Å^{-2}]	σ [Å]
digitonin				44.8	7.4	5.9
outer head group	12.9	11.9	4.1	10.1	9.1	4.2
alkyl chain	25.6	8.0	3.9	27.3	6.8	3.4
inner head group	10.1	11.8	3.9	10.1	9.7	3.2
water	3.1	9.4	3.3	3.3	9.4	3.4
SiO_2	10.1	18.6	3.4	10.1	18.6	3.4

A decrease in the SLD of the outer head group layer from 11.9×10^{-6} to 9.1×10^{-6} Å^{-2} as well as in the SLD of the alkyl chain layer from 7.3×10^{-6} to 6.8×10^{-6} Å^{-2} suggests that digitonin does not only adsorb on the membrane surface but

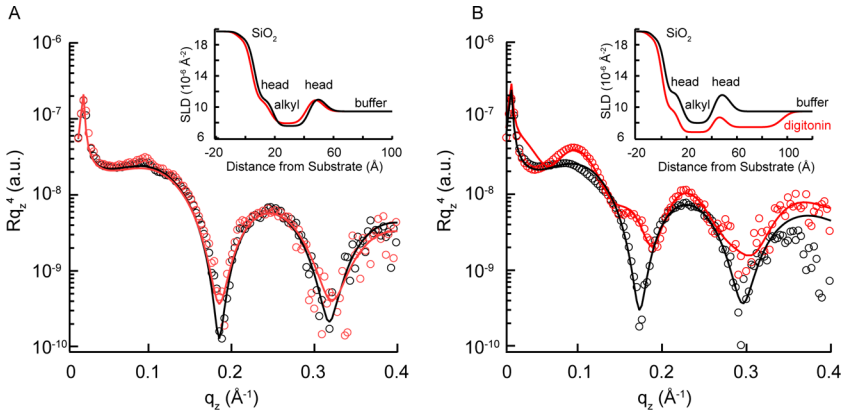

Figure 3. Fine structures of supported membranes investigated by high-energy specular XRR. (A) XRR of a pure SOPC membrane in the absence (black) and presence (red) of 50 μM digitonin. (B) XRR of a SOPC membrane incorporating 20 mol % cholesterol in the absence (black) and presence (red) of 50 μM digitonin. The experimental errors are within the symbol size. The solid lines represent the best model fits to the data. The scattering length density (SLD) profiles corresponding to the best-fit results are presented in the insets.

dx.doi.org/10.1021/jp5074939 | J. Phys. Chem. B 2014, 118, 14632–14639

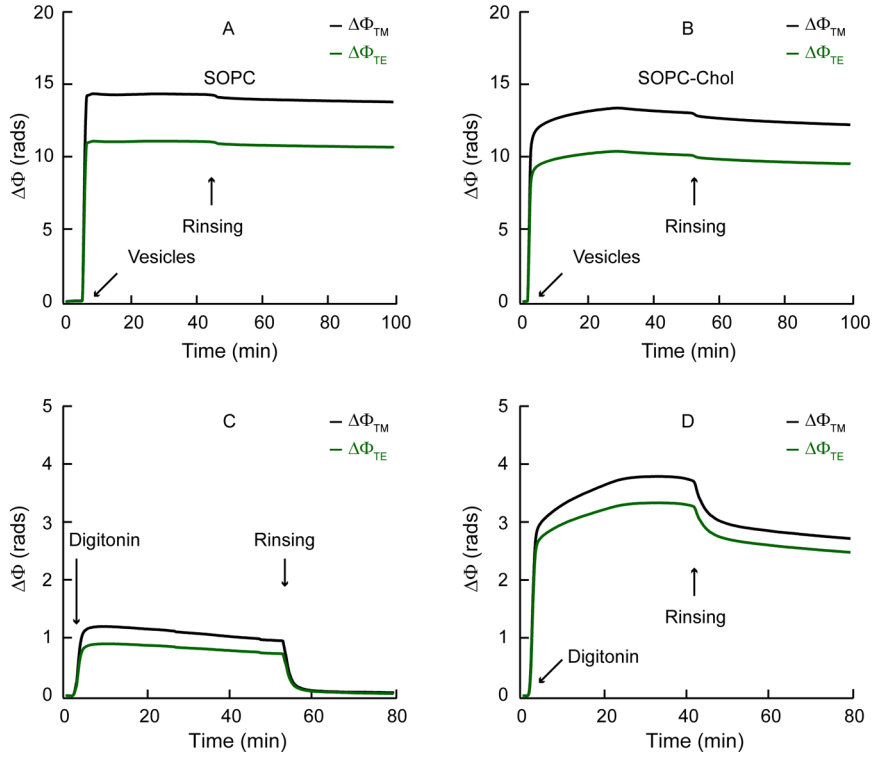

Figure 4. Real-time phase changes in TM and TE waveguide modes $\Delta\Phi_{TM}$ (black) and $\Delta\Phi_{TE}$ (green) of (A) a pure SOPC membrane and (B) a SOPC membrane incorporating 20 mol % cholesterol prior to the incubation with digitonin, confirming the formation of supported membranes. The injection of 50 μM digitonin resulted in a minor phase shift in the case of the pure SOPC membrane (C), while the membrane with cholesterol exhibited a pronounced phase shift even after rigorous rinsing (D).

also removes some molecules from the membrane. This could be attributed to the formation of digitonin−cholesterol complexes reported previously.[14,34] The thickness of the digitonin layer ($d \approx 45$ Å) roughly corresponds to the double of the molecular length of digitonin ($l \approx 20$ Å), and its high SLD value (7.4×10^{-6} Å^{-2}) suggests that this layer consists of dense aggregates of sterol and aglycone. Last but not least, the formation of a digitonin layer possessing a roughness of $\sigma \approx 6$ Å causes no significant change in the roughness of the other interfaces. Our fine structural analysis has demonstrated for the first time that digitonin does not destroy the structural integrity of membranes, which is in clear contrast to the previous studies suggesting the destruction of membranes by the formation of defects or surface micelles.[12,14]

DPI. DPI measurements were performed in order to gain further insights into changes in the structures of supported membranes caused by digitonin. In addition to the parameters obtained by the reflectivity-based techniques (e.g., ellipsometry and XRR), such as thickness d and refractive index n, DPI also yields the change in the mass density Δm_{DPI}. It should be noted that the change in the mass measured by QCM-D $\Delta m_{QCM\text{-}D}$ includes the mass of hydrating water, while DPI complementarily yields the change in the mass of dry components. Another unique quantity that one can gain from the DPI is birefringence $\Delta n = n_0 - n_e$, which is the difference between the ordinary and extraordinary refractive indices. In the case of supported membranes, Δn can be used as a measure for the ordering of alkyl chains.[35,36]

Figure 4 represents the raw phase data of a pure SOPC membrane and a SOPC membrane incorporating 20 mol % cholesterol in the absence and presence of 50 μM digitonin, and the best-fit results for the SOPC membrane incorporating 20 mol % cholesterol are presented in Table 4.

Table 4. Best-Fit Parameters for the DPI Results for the SOPC Membrane Incorporating 20 mol % Cholesterol in the Absence and Presence of 50 μm Digitonin

layer	RI	d (Å)	birefringence	Δm_{DPI} (ng/cm^2)	$\Delta\rho$ (g/cm^3)
digitonin	1.36	45[a]	0	70 ± 7	0.15 ± 0.01
SOPC−chol	1.45	47[a]	0.01	377 ± 5	0.80 ± 0.01

[a]A constant thickness obtained from XRR was taken for the calculation.

Figure 4A and B illustrates the real-time phase changes in TM and TE waveguide modes $\Delta\Phi_{TM}$ (black) and $\Delta\Phi_{TE}$ (green) during the formation of a pure SOPC and a SOPC membrane incorporating 20 mol % cholesterol, respectively. An increase in phase ($\Delta\Phi_{TM}^{SOPC} \approx 14$ rad, $\Delta\Phi_{TE}^{SOPC} \approx 11$ rad, and $\Delta\Phi_{TM}^{SOPC-chol} \approx 13$ rads, $\Delta\Phi_{TE}^{SOPC-chol} \approx 9$ rads) suggests the formation of a supported lipid bilayer.[36] The parameters of membranes with cholesterol are slightly different from those obtained from pure SOPC membranes, which can be attributed to the fact that alkyl chains take a liquid-ordered phase in the presence of cholesterol.

The injection of a 50 μM digitonin solution to the pure SOPC membrane (Figure 5C) caused a slight change in phase, but the signal came back to the initial level after rinsing with PBS buffer ($\Delta\Phi^{SOPC} \approx 0.1$ rad). This finding seems consistent with the other results (QCM-D, XRR), suggesting that pure SOPC membranes remain intact even in the presence of 50 μM

dx.doi.org/10.1021/jp5074939 | J. Phys. Chem. B 2014, 118, 14632−14639

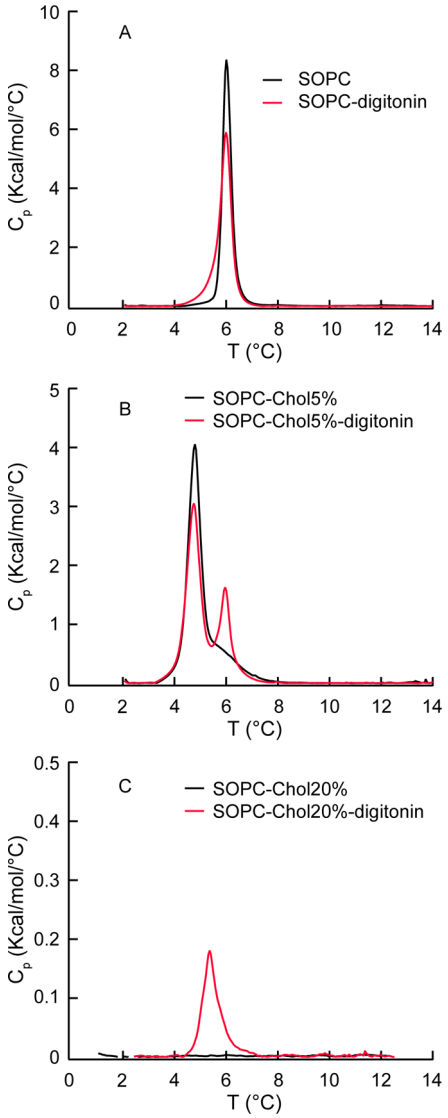

Figure 5. DSC scans of SOPC liposomes with 0 (A), 5 (B), and 20 mol % (C) cholesterol in the absence (black) and presence (red) of 50 μM digitonin.

digitonin. In contrast, the injection of digitonin to the SOPC membrane incorporating 20 mol % cholesterol (Figure 5D) led to a more pronounced increase in phase. Here, the final phase shift rinsing with PBS buffer ($\Delta\Phi_{TM}^{SOPC-chol} \approx 2.7$ rad; $\Delta\Phi_{TE}^{SOPC-chol} \approx 2.5$ rad) was distinctly higher than the original level.

To gain the structural parameters of the layer formed by the injection of digitonin, the thickness of the lipid membrane was fixed at $d = 47 \pm 2$ Å, taking the value obtained by XRR. We found that the injection of digitonin led to a significant increase in the mass ($\Delta m_{DPI} = 70 \pm 7$ ng/cm^2) as well as in the average density ($\Delta\rho = 0.15 \pm 0.01$ g/cm^3). Taking Δm obtained by QCM-D ($\Delta m_{QCM\text{-}D} = 685 \pm 47$ ng/cm^2), the fraction of the hydrating water H (in wt %) can be calculated as

$$H = \frac{m_{water}}{m_{acoustic}} = \frac{m_{QCM\text{-}D} - m_{DPI}}{m_{QCM\text{-}D}} \times 100 \approx 90 \text{ wt \%}$$

This result seems consistent with the shear viscosity and shear modulus values, which are close to those of water (Table 1).

Effect of Digitonin on Membrane Thermodynamics. As presented in Table 3, XRR implied that the SLD of alkyl chains decreased when the membrane was in contact with digitonin, suggesting that digitonin molecules do not only adsorb onto the membrane surface but also remove cholesterol from the membrane core. However, it is technically almost impossible to quantitatively assess the significance of digitonin−cholesterol interactions. For this purpose, we investigated the thermotropic phase diagrams of membranes using a differential scanning calorimeter (DSC). Figure 6 shows

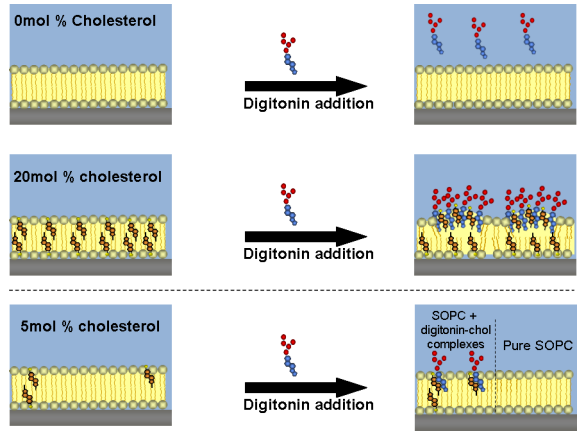

Figure 6. Interactions of digitonin with phospholipid membranes incorporating cholesterol.

DSC scans of SOPC membranes incorporating (A) 0, (B) 5, and (C) 20 mol % cholesterol in the absence (black) and presence (red) of 50 μM of digitonin. The DSC thermograms of cholesterol-containing liposomes were significantly altered in the presence of digitonin. As presented in Figure 5A, the DSC scan of pure SOPC membranes (black) exhibited a very sharp endothermic peak at $T_m = 6.0$ °C and $\Delta H = 3.9$ kcal/mol, corresponding to the main thermotropic transition from the gel phase to the liquid crystalline phase. In the presence of digitonin (red), the transition temperature remained almost identical, but the onset of the phase transition appeared at a slightly lower temperature. Nevertheless, the broadening of the transition peak and the decrease in the transition enthalpy remained below 6%, suggesting that the pure SOPC membranes remain almost intact in the presence of 50 μM digitonin.

A SOPC membrane incorporating 5 mol % cholesterol (Figure 5B, black) showed the main peak at 4.8 °C accompanied by a subpeak (shoulder) at around 6.0 °C, and the transition enthalpy decreased to $\Delta H = \int C_p \, dT = 3.5$ kcal/mol. This finding suggests a partial mixing of SOPC and substitutional impurity (cholesterol). Namely, the major peak at 4.8 °C coincides with the transition of the SOPC−cholesterol complex, while the one at 6.0 °C coincides with the transition of SOPC. The presence of 50 μM digitonin (Figure 5B, red) resulted in a remarkable change in the weight balance between these two peaks. Indeed, whereas the first peak decreases, the second peak becomes sharper. This finding implies that the increase in the ratio of the pure SOPC fraction and hence the decrease in the SOPC−cholesterol complex due to the partial removal of cholesterol by digitonin.

When the molar fraction of cholesterol increased to 20 mol % (Figure 5C, black), the endothermic peak diminished due to

dx.doi.org/10.1021/jp5074939 | J. Phys. Chem. B 2014, 118, 14632−14639

the formation of another monophase, called the liquid-ordered phase, where alkyl chains are ordered but do not take an all-trans conformation because cholesterol acts as the substitutional impurity.[37] It was highly remarkable that an endothermic peak at 5.4 °C appeared in the presence of digitonin (Figure 5C, red). The "recovery" of an endothermic peak observed here could be interpreted as the removal of cholesterol molecules by digitonin. Although the exact number of molecules forming a complex unit could not be determined, the new peak coincides with the phase transition of the SOPC−cholesterol complex with a different coordinate number from what we observed at 5 mol %. In fact, a relatively broad (fwhm = 0.6 °C), asymmetric peak that we observed suggests the dispersion of coordination numbers.[37]

Our experimental finding qualitatively agrees well with the previous study that reported a lateral phase separation of DPPC−cholesterol mixtures by the combination of DSC and fluorescence anisotropy measurements.[14]

CONCLUSIONS

The aim of the present work was to assess the mechanism of interaction between digitonin and cholesterol-containing membranes in a quantitative manner. To do so, we used defined membrane models in the presence or absence of cholesterol and analyzed the mechanism of interaction with digitonin at a nominal concentration of 50 μM (C < CMC), which is usually used for cells or erythrocytes lysis. We have demonstrated that the combination of defined membrane models and physical techniques enables us to gain mechanistic insights into the interaction mechanisms between digitonin and model cell membranes in a quantitative manner (Figure 6).

In the case of the pure SOPC membrane, the membrane remained almost intact in the presence of 50 μM digitonin (Figure 6A). No increase in the mass density or shear modulus could be detected by QCM-D (Figure 1C). High-energy XRR (Figure 3A) suggested no remarkable change in the membrane thickness, SLD, and roughness of all of the slabs (Table 2). Moreover, no significant change in phase could be detected by the DPI (Figure 4C), suggesting that the SOPC membrane was not altered by digitonin. This was further confirmed by DSC, demonstrating that digitonin does not influence the thermotropic phase transition of SOPC membranes (Figure 5A).

In contrast, digitonin strongly interacts with SOPC membranes incorporating 20 mol % cholesterol (Figure 6B). Distinct changes in both resonant frequency Δf_n and dissipation ΔD (Figure 1D) could be detected by QCM-D. The experimental results could be well interpreted with the Voigt model (Figure 2), yielding the formation of a viscoelastic layer on the membrane surface. The fine structural analysis with high-energy XRR (Figure 3B, Table 3) also suggested that digitonin does not cause significant membrane destruction but leads to the removal of cholesterol from the membrane core, which could be identified by a slight decrease in SLD. The XRR results could well be interpreted as the formation of an additional slab with a thickness of 45 Å possessing a larger roughness at the outermost interface with the bulk. To further verify if cholesterol is removed from the membrane core by the formation of digitonin−cholesterol complexes, we performed DSC experiments. The obtained result (Figure 5B) clearly indicated the reappearance of the main phase transition of SOPC, which can be explained by the removal of substitutional impurities (cholesterol molecules) that initially suppressed the phase transition by sustaining the system at the liquid-ordered phase. This was further verified by the experiments with membranes incorporating 5 mol % cholesterol. On the basis of the obtained results, we suggest the following mechanism of interaction between digitonin and cholesterol molecules in the SOPC−cholesterol bilayers (Figure 6). First, digitonin molecules penetrate into the membrane containing cholesterol and then bind to cholesterol molecules. The formation of sterol−aglycone aggregates does not lead to any significant membrane destruction, but cholesterols are removed from the hydrophobic core region (Figure 6). Finally, the sterical hindrance between saccharide residues in these aggregates may induce changes in the curvature of the membrane outer leaflet, leading thus to an increase in the membrane permeability.

The obtained results suggest that the combination of QCM-D, high-energy XRR, DPI, and DSC provides us with a powerful tool to unravel the mechanism of interaction between molecules with low molecular weights and cell membrane models, which could not be assessed otherwise.

AUTHOR INFORMATION

Corresponding Authors

*E-mail: wink@uni-heidelberg.de (M.W.).
*E-mail: tanaka@uni-heidelberg.de (M.T.).

Present Address

[⊥](A.M.) CNRS UMR 8612, Institut Galien Paris-Sud, Faculté de Pharmacie, 5 rue J.B. Clément, 92296 Châtenay-Malabry, France.

Author Contributions

[#]N.F. and A.M. contributed equally.

Notes

The authors declare no competing financial interest.

ACKNOWLEDGMENTS

This work was supported by the Helmholtz Association (BioInterfaces Program) and JSPS (No. 26247070). We thank M. Swan and W. Abuillan for helpful discussion. N.F. thanks the Studienstiftung des Deutschen Volkes e.V., Baden Württemberg Stiftung (BWS-Plus), and BioInterfaces International Graduate School. A.M. is thankful to the Alexander von Humboldt Foundation for the postdoctoral fellowship. M.T. is a member of German Excellence Cluster "Cell Networks". iCeMS is supported by the World Premier International Research Center Initiative (WPI), MEXT, Japan.

REFERENCES

(1) Keukens, E. A.; de Vrije, T.; Fabrie, C. H.; Demel, R. A.; Jongen, W. M.; de Kruijff, B. Dual Specificity of Sterol-Mediated Glycoalkaloid Induced Membrane Disruption. *Biochim. Biophys. Acta* **1992**, *1110*, 127−136.

(2) Hostettmann, K.; Marston, A. *Chemistry and Pharmacology of Natural Products: Saponins*; Cambridge University Press: New York, 1995.

(3) De Geyter, E.; Smagghe, G.; Rahbe, Y.; Geelen, D. Triterpene Saponins of Quillaja Saponaria Show Strong Aphicidal and Deterrent Activity against the Pea Aphid Acyrthosiphon Pisum. *Pest Manage. Sci.* **2012**, *68*, 164−169.

(4) Thakur, M.; Melzig, M. F.; Fuchs, H.; Weng, A. Chemistry and Pharmacology of Saponins: Special Focus on Cytotoxic Properties. *Botanics: Targets Therapy* **2011**, 19−29.

(5) Wink, M.; van Wyk, B.-E. *Mind-Altering and Poisonous Plants of the World*; Timber Press: London, 2008.

(6) Liu, J.; Xiao, N.; DeFranco, D. B. Use of Digitonin-Permeabilized Cells in Studies of Steroid Receptor Subnuclear Trafficking. *Methods Enzymol.* **1999**, *19*, 403−409.
(7) Fiskum, G.; Craig, S. W.; Decker, G. L.; Lehninger, A. L. The Cytoskeleton of Digitonin-Treated Rat Hepatocytes. *Proc. Natl. Acad. Sci. U.S.A.* **1980**, *77*, 3430−3434.
(8) Akiyama, T.; Takagi, S.; Sankawa, U.; Inari, S.; Saito, H. Saponin−Cholesterol Interaction in the Multibilayers of Egg Yolk Lecithin as Studied by Deuterium Nuclear Magnetic Resonance: Digitonin and Its Analogues. *Biochemistry* **1980**, *19*, 1904−1911.
(9) Yu, B.; Choi, H. The Effects of Digitonin and Glycyrrhizin on Liposomes. *Arch. Pharmacal Res.* **1986**, *9*, 119−125.
(10) Murphy, E.; Coll, K.; Rich, T. L.; Williamson, J. R. Hormonal Effects on Calcium Homeostasis in Isolated Hepatocytes. *J. Biol. Chem.* **1980**, *255*, 6600−6608.
(11) Zuurendonk, P. F.; Tager, J. M. Rapid Separation of Particulate Components and Soluble Cytoplasm of Isolated Rat-Liver Cells. *Biochim. Biophys. Acta* **1974**, *333*, 393−399.
(12) Stearns, M. E.; Ochs, R. L. A Functional In Vitro Model for Studies of Intracellular Motility in Digitonin-Permeabilized Erythrophores. *J. Cell Biol.* **1982**, *94*, 727−739.
(13) Fischer, A. H.; Jacobson, K. A.; Rose, J.; Zeller, R. Fixation and Permeabilization of Cells and Tissues. *Cold Spring Harb. Protoc.* **2008**, DOI: 10.1101/pdb.top36.
(14) Nishikawa, M.; Nojima, S.; Akiyama, T.; Sankawa, U.; Inoue, K. Interaction of Digitonin and Its Analogs with Membrane Cholesterol. *J. Biochem.* **1984**, *96*, 1231−1239.
(15) Goegelein, H.; Hueby, A. Interaction of Saponin and Digitonin with Black Lipid Membranes and Lipid Monolayers. *Biochim. Biophys. Acta* **1984**, *773*, 32−38.
(16) Golemanov, K.; Tcholakova, S.; Denkov, N.; Pelan, E.; Stoyanov, S. D. Remarkably High Surface Visco-Elasticity of Adsorption Layers of Triterpenoid Saponins. *Soft Matter* **2013**, *9*, 5738−5752.
(17) Sackmann, E. Supported Membranes: Scientific and Practical Applications. *Science* **1996**, *271*, 43−48.
(18) Tanaka, M.; Sackmann, E. Polymer-Supported Membranes as Models of the Cell Surface. *Nature* **2005**, *437*, 656−663.
(19) Bangham, A. D.; Standish, M. M.; Watkins, J. C. Diffusion of Univalent Ions across the Lamellae of Swollen Phospholipids. *J. Mol. Biol.* **1965**, *13*, 238−252.
(20) Makky, A.; Michel, J. P.; Ballut, S.; Kasselouri, A.; Maillard, P.; Rosilio, V. Effect of Cholesterol and Sugar on the Penetration of Glycodendrimeric Phenylporphyrins into Biomimetic Models of Retinoblastoma Cells Membranes. *Langmuir* **2010**, *26*, 11145−11156.
(21) Sauerbrey, G. Verwendung von Schwingquarzen zur Wägung Dünner Schichten und zur Mikrowägung. *Z. Phys.* **1959**, *155*, 206−222.
(22) Voinova, M. V.; Rodahl, M.; Jonson, M.; Kasemo, B. Viscoelastic Acoustic Response of Layered Polymer Films at Fluid−Solid Interfaces: Continuum Mechanics Approach. *Phys. Scr.* **1999**, *59*, 391.
(23) Parratt, L. G. Surface Studies of Solids by Total Reflection of X-rays. *Phys. Rev.* **1954**, *95*, 359.
(24) Tolan, M. *X-ray Scattering from Soft-Matter Thin Films*; Springer: Berlin, Heidelberg, Germany, 1999.
(25) Nelson, A. Co-Refinement of Multiple-Contrast Neutron/X-ray Reflectivity Data Using Motofit. *J. Appl. Crystallogr.* **2006**, *39*, 273−276.
(26) Cowsill, B. J.; Coffey, P. D.; Yaseen, M.; Waigh, T. A.; Freeman, N. J.; Lu, J. R. Measurement of the Thickness of Ultra-Thin Adsorbed Globular Protein Layers with Dual-Polarisation Interferometry: A Comparison with Neutron Reflectivity. *Soft Matter* **2011**, *7*, 7223−7230.
(27) Cross, G. H.; Reeves, A. A.; Brand, S.; Popplewell, J. F.; Peel, L. L.; Swann, M. J.; Freeman, N. J. A New Quantitative Optical Biosensor for Protein Characterisation. *Biosens. Bioelectron.* **2003**, *19*, 383−390.
(28) Cross, G. H.; Ren, Y. T.; Freeman, N. J. Young's Fringes from Vertically Integrated Slab Waveguides: Applications to Humidity Sensing. *J. Appl. Phys.* **1999**, *86*, 6483−6488.
(29) Keller, C. A.; Glasmästar, K.; Zhdanov, V. P.; Kasemo, B. Formation of Supported Membranes from Vesicles. *Phys. Rev. Lett.* **2000**, *84*, 5443−5446.
(30) Larsson, C.; Rodahl, M.; Hook, F. Characterization of DNA Immobilization and Subsequent Hybridization on a 2D Arrangement of Streptavidin on a Biotin-Modified Lipid Bilayer Supported on SiO_2. *Anal. Chem.* **2003**, *75*, 5080−5087.
(31) Malmstrom, J.; Agheli, H.; Kingshott, P.; Sutherland, D. S. Viscoelastic Modeling of Highly Hydrated Laminin Layers at Homogeneous and Nanostructured Surfaces: Quantification of Protein Layer Properties Using QCM-D and SPR. *Langmuir* **2007**, *23*, 9760−9768.
(32) Lipowsky, R.; Sackmann, E. *Structure and Dynamics of Membranes*; Elsevier Science Limited: New York, 1995; Vol *1*, Parts A and B.
(33) Reich, C.; Horton, M. R.; Krause, B.; Gast, A. P.; Radler, J. O.; Nickel, B. Asymmetric Structural Features in Single Supported Lipid Bilayers Containing Cholesterol and GM1 Resolved with Synchrotron X-ray Reflectivity. *Biophys. J.* **2008**, *95*, 657−668.
(34) Windaus, A. Über die Entgiftung der Saponine durch Cholesterin. *Ber. Dtsch. Chem. Ges.* **1909**, *42*, 238−246.
(35) Lee, T.-H.; Hall, K. N.; Swann, M. J.; Popplewell, J. F.; Unabia, S.; Park, Y.; Hahm, K.-S.; Aguilar, M.-I. The Membrane Insertion of Helical Antimicrobial Peptides from the N-Terminus of Helicobacter Pylori Ribosomal Protein L1. *Biochim. Biophys. Acta* **2010**, *1798*, 544−557.
(36) Mashaghi, A.; Swann, M.; Popplewell, J.; Textor, M.; Reimhult, E. Optical Anisotropy of Supported Lipid Structures Probed by Waveguide Spectroscopy and Its Application to Study of Supported Lipid Bilayer Formation Kinetics. *Anal. Chem.* **2008**, *80*, 3666−3676.
(37) Cevc, G. *Phospholipids Handbook*; CRC Press: New York, 1993.